

Dissociative excitation of HeH^+ by electron impact

A. E. Orel

Department of Applied Science, University of California, Davis, Livermore, California 94550

T. N. Rescigno and B. H. Lengsfeld III

Lawrence Livermore National Laboratory, P. O. Box 808, Livermore, California 94550

(Received 11 March 1991)

We report the results of an *ab initio* variational treatment of electron-impact cross sections for the process $e^- + \text{HeH}^+ \rightarrow e^- + \text{He}^+ + \text{H}$ for electron energies between 21 eV, the threshold for excitation of the dissociative $1^3\Sigma^+$ state, and 26 eV, corresponding to the excitation energy of the first $1^3\Sigma^+$ excited state. The calculations, which were carried out using a recent modification of the complex Kohn method, employed accurate correlated target wave functions, as well as *ab initio* optical potentials to incorporate the effect of closed channels. The fixed-nuclei excitation cross sections were found to be dominated by a series of sharp resonance structures. However, when the cross sections are averaged over the Franck-Condon envelope of the ground vibrational state, these sharp features are no longer seen. We conclude that the recent experiments that report structure in the HeH^+ dissociation cross section cannot be explained within the context of traditional adiabatic-nuclei theory.

PACS number(s): 34.80.Gs

I. INTRODUCTION

Yousif and Mitchell [1] have recently carried out merged-beam studies of dissociative recombination of HeH^+ with electrons. In the 21–26-eV energy range, dissociation of ground-state HeH^+ into $\text{He}^+ + \text{H}$ can only proceed via excitation of the repulsive $1^3\Sigma^+$ state. The experimentally measured cross section for this process displayed sharp peaks near the excitation threshold as well as near the threshold for exciting the next excited $1^3\Sigma^+$ state at 26 eV. These peaks were superimposed on a flat background that appears to be negligibly small on the scale of the measurements. Yousif and Mitchell postulated several possible explanations for the observed structures, the most likely being doubly excited autoionizing states. These interesting measurements prompted us to carry out a detailed study of $e^- + \text{HeH}^+$ scattering in the 21–26-eV energy range, to elucidate the nature of the resonance peaks and to quantify the magnitude of the background dissociation cross section. To accomplish this task, we used the complex Kohn variational method [2], recently modified to handle electron collisions with ionic molecular targets [3]. The variational calculations employed a many-electron trial wave function built from accurate multiconfiguration target states. We also con-

structed fully *ab initio* optical potentials to incorporate electron-target correlation and closed-channel effects which are critical in determining the resonance structure in the excitation cross section.

In the following section, we will outline the theoretical procedures we have used in this study. In Sec. III we describe the details of our calculations and present results. We conclude with a brief discussion.

II. THEORY

Detailed descriptions of the complex Kohn variational method and the way it is implemented to study e^- -molecule collisions have been given previously [2–5] and will not be repeated here. We will limit ourselves to a brief summary of the salient points and concentrate instead on those aspects of the implementation needed when multiconfiguration target state wave functions are used as well as technical details which have not been previously delineated.

A. Complex Kohn variational method

The trial wave function we use is of the standard “close coupling plus correlation” form [6–8]:

$$\Psi_{\Gamma_0}(r_1, r_2, \dots, r_{N+1}) = \sum_{\Gamma} \mathcal{A}(\chi_{\Gamma}(r_1, r_2, \dots, r_N) F_{\Gamma\Gamma_0}(r_{N+1})) + \sum_{\mu} d_{\mu}^{\Gamma_0} \Theta_{\mu}(r_1, r_2, \dots, r_{N+1}) \quad (1)$$

where the first sum runs over the energetically open target states χ_{Γ} , $F_{\Gamma\Gamma_0}$ is a one-electron channel orbital antisymmetrized to χ_{Γ} by the operator \mathcal{A} , and Θ_{μ} is an $(N+1)$ -electron configuration state function built from square-integrable functions. The index Γ_0 denotes a par-

ticular degenerate solution labeled by the electron incident on the target in state χ_{Γ_0} . In the complex Kohn method the channel functions $F_{\Gamma\Gamma_0}$ are expanded as linear combinations of short-ranged functions φ_k^{Γ} , as well as outgoing continuum functions g_l^{Γ} and regular continu-

um functions f_l^Γ , the latter fixed with unit coefficients in channel Γ_0 :

$$F_{\Gamma\Gamma_0}(r) = \sum_{l,m} [f_l^\Gamma(r)\delta_{ll_0}\delta_{mm_0}\delta_{\Gamma\Gamma_0} + T_{lm_l_0m_0}^{\Gamma\Gamma_0}g_l^\Gamma(r)] \times Y_{lm}(\hat{\mathbf{r}})/r + \sum_k c_k^{\Gamma\Gamma_0}\varphi_k^\Gamma(r), \quad (2)$$

with

$$f_l^\Gamma(r) \underset{r \rightarrow \infty}{\sim} \frac{\sin(\rho_\Gamma - \eta_\Gamma \ln 2\rho_\Gamma - l\pi/2 + \sigma_l^\Gamma)}{(k_\Gamma)^{1/2}}, \quad (3)$$

$$g_l^\Gamma(r) \underset{r \rightarrow \infty}{\sim} \frac{\exp[i(\rho_\Gamma - \eta_\Gamma \ln 2\rho_\Gamma - l\pi/2 + \sigma_l^\Gamma)]}{(k_\Gamma)^{1/2}}$$

where $\rho_\Gamma = k_\Gamma r$, $\eta_\Gamma = Z/k_\Gamma$, $\sigma_l^\Gamma = \arg[\Gamma(1+l+i\eta_\Gamma)]$, and k_Γ is a channel momentum.

The ‘‘conventional’’ choice for the continuum basis functions is simply to use regular and outgoing-wave Coulomb functions, the latter suitably regularized at the origin with some arbitrary cutoff function. We have noticed [9] that for ionic targets, there can be quite a bit of sensitivity to the form of the cutoff used and that convergence and stability is greatly enhanced by choosing the outgoing continuum function instead as

$$g_l^\Gamma(r) = \mathcal{G}_l^{+c} V / \int V F_l \quad (4)$$

where \mathcal{G}_l^{+c} is the partial-wave Coulomb Green’s function, V is any short-range function (we use a simple exponential), and F_l is the regular Coulomb function. It is simple to show that this function satisfies the asymptotic form specified in Eq. (3). The physical motivation for this choice of continuum basis, as well as numerical details about its construction, are outlined in Ref. [9]. It is interesting to note that this choice makes the method quite similar to the scattered wave variational method proposed by Sun *et al.* [10] for reactive scattering.

The coefficients $T_{lm_l_0m_0}^{\Gamma\Gamma_0}$ of Eq. (2) are elements of the T matrix from which cross sections are constructed. These coefficients, along with the parameters $c_k^{\Gamma\Gamma_0}$, are determined by making the Kohn functional,

$$[T^{\Gamma\Gamma_0}] = T^{\Gamma\Gamma_0} - 2 \int \Psi_\Gamma (H - E) \Psi_{\Gamma_0}, \quad (5)$$

stationary and solving the resulting set of linear equations [11]. Note that our definition of the T matrix is such that for single channel scattering from a spherically symmetric potential, $T_{lm_l'm'} = \delta_{ll'}\delta_{mm'}e^{i\delta_l'}\sin\delta_l'$. Much of the computational effort is involved in building matrix elements of the many-electron Hamiltonian over the various pieces of the trial wave function. Since the viability of the entire approach depends critically on the ease with which these matrix elements can be assembled, we take advantage of a variety of computational techniques aimed at simplifying the process. These techniques are delineated in the following sections.

B. P- and Q-space partitioning

It is convenient to partition the total wave function into two parts, $P\psi_\Gamma$ and $Q\psi_\Gamma$, corresponding to the two

sums defined in Eq. (1). Since $Q\psi_\Gamma$ is square integrable, it is not explicitly needed for the determination of scattering parameters. As we previously stated, the channel orbitals $F_{\Gamma\Gamma_0}$ in the Kohn method are expanded as linear combinations of bound and continuum functions. All these functions can be mutually orthogonalized without changing the resulting T matrix, a property known as transfer invariance [11–13]. We also follow the common practice of requiring the channel orbitals to be orthogonal to all the bound-state orbitals which are used to form the target wave functions [6]. This latter requirement may introduce constraints which must be relaxed by the addition of appropriate $(N+1)$ -electron terms to $Q\psi$. We will have more to say about this below.

$P\psi$ is restricted in our formulation to include only open-channel terms. Therefore, any closed-channel effects one may wish to include such as electron-target correlation or target polarization must be incorporated into the terms used to expand $Q\psi$. It is important to note, then, that the configuration state functions $\{\Theta_\mu\}$ from which $Q\psi$ is built are of two distinct types. One class of terms is needed to relax any unphysical constraints placed on the total wave function by the requirement that the channel scattering orbitals be orthogonal to the target basis orbitals. To add to the confusion, some authors refer to these as short-range correlation terms. We will refer to these as ‘‘orthogonality relaxing’’ or ‘‘penetration’’ terms [14]. These terms are, in general, always needed except in cases where space or spin considerations eliminate them. If the scattering orbitals were not constrained to be orthogonal to the target orbitals, these terms would not be needed, but the formalism would be considerably more cumbersome. The other class of terms in $\{\Theta_\mu\}$ represents the effect of closed channels and target polarization.

In calculations which include the effect of closed channels, the set of Q -space configurations can become quite large. For this reason, and because of the fact that the configuration state functions $\{\Theta_\mu\}$ are built solely from square-integrable orbitals, it is desirable to use bound-state molecular structure methods to treat the Q -space portion of the problem and to divorce this part of the calculation from the rest of the variational calculation. This can be done by using Feshbach partitioning [15].

Defining M as $H - E$, we can derive in the usual way [11] a modified Hamiltonian that determines $P\psi$:

$$H_{\text{eff}} = H_{PP} + M_{PQ}M_{QQ}^{-1}M_{QP} \\ = H_{PP} + V_{\text{opt}} \quad (6)$$

where M_{QQ}^{-1} is the inverse of the Hamiltonian matrix spanned by the functions $\{\Theta_\mu\}$. This allows us to drop the variational coefficients $d_{\mu}^{\Gamma_0}$ in Eq. (1) from further consideration. Note that it is not actually necessary to invert M_{QQ} to construct the effective Hamiltonian. If Q space is very large, it is preferable to solve the set of linear equations

$$M_{QQ}X = M_{QP} \quad (7)$$

and then construct $M_{PQ}X$ to produce the desired optical

als. We now turn our attention to the second class of Q -space configurations which are used to include the effects of closed channels.

Recall that the P -space vectors were constructed as direct products of scattering orbitals and a fixed number m of eigenstates of an $n \times n$ Hamiltonian matrix. The complement of P space consists of the direct product of the scattering orbitals and the remaining $(n - m)$ target eigenstates, which are presumed to be energetically closed. Thus the complement of P space can be used to generate Q -space configurations which describe the effect of closed channels. Which closed channels are included will of course depend upon the number and type of configurations included in $\{\Phi\}$. In the remainder of this paper we will refer to these Q -space configurations as CI relaxation terms.

In order to provide a complete discussion of this topic, we note that additional closed channels can also be incorporated in the scattering problem by adding terms in Q space which are the direct product of a scattering function and a linear combination of a disjoint set of configurations. These configurations were not included in the CI expansion used to determine the target wave functions and are introduced, for example, in low-energy scattering problems to incorporate polarization effects in the trial wave functions. These disjoint linear combinations of configurations must be noninteracting with the target wave functions,

$$\langle \Psi^d | H | \Psi_{\Gamma}^{\text{target}} \rangle \text{ for all } \Gamma, \quad (12)$$

and this constraint restricts the introduction of this class of closed-channel terms to problems where all of the open channels possess different spin or spatial symmetry properties. This class of polarization terms has been used in recent studies of low-energy electron-methane [18] and electron-silane scattering [19].

In this study, only penetration terms and CI relaxation terms are included in Q space. The algorithm that is used to include the CI relaxation terms in Q space does *not* require the determination of all of the eigenvectors of the target Hamiltonian. Rather, we employ projection operators to account for these terms and can thereby avoid the explicit construction of H_{QQ} . In building the optical potential discussed in the preceding section of this work, H_{QQ} is used to solve a set of linear equations,

$$H_{QQ} X_{QP} = H_{QP} \quad (13)$$

and

$$V_{PP}^{\text{opt}} = H_{PQ} X_{QP}. \quad (14)$$

This equation is solved in the configuration state function basis rather than in the basis of CI eigenfunctions [20]. Thus

$$\begin{aligned} H_{QQ} &= \begin{pmatrix} 1 - |C_p\rangle \langle C_p| & 0 \\ 0 & 1 \end{pmatrix} \begin{pmatrix} H_{ij}^{kl} & H_{iq}^k \\ H_{iq}^{k\dagger} & H_{qq} \end{pmatrix} \begin{pmatrix} |1 - |C_p\rangle \langle C_p| & 0 \\ 0 & 1 \end{pmatrix} \\ &\equiv \rho_Q \begin{pmatrix} H_{ij}^{kl} & H_{iq}^k \\ H_{iq}^{k\dagger} & H_{qq} \end{pmatrix} \rho_Q \\ &\equiv \rho_Q H_{QQ}^{\text{CSF}} \rho_Q. \end{aligned} \quad (15)$$

The linear equations, Eq. (13), are solved iteratively by successively multiplying H_{QQ} by a set of trial vectors (X^i , $i = 1, \dots, r$) and solving a small set of linear equations in the trial space until convergence is achieved. This type of algorithm has been discussed in a number of papers [21] and a detailed description will not be given here. We only note that neither the projection operator ρ_Q nor the Q -space Hamiltonian H_{QQ}^{CSF} need be explicitly constructed [20]. The multiplication of a trial vector X^i by H_{QQ} is conducted in a series of vectorizable steps:

$$\begin{aligned} \rho_Q X^i &= (1 - |C_p\rangle \langle C_p|) |X^i\rangle \\ &= |X^i\rangle - |C_p\rangle \langle C_p | X^i \rangle \\ &\equiv X_p^i, \end{aligned} \quad (16a)$$

$$H_{QQ}^{\text{CSF}} X_p^i = R_Q^i, \quad (16b)$$

$$\rho_Q R_Q^i = |R_Q^i\rangle - |C_p\rangle \langle C_p | R_Q^i \rangle. \quad (16c)$$

A direct-CI procedure can be used to perform the multiplication of H_{QQ}^{CSF} times the projected trial function. This is a standard procedure in most modern electronic structure packages [16] and allows us to employ large Hamiltonian matrices in the scattering calculations.

This discussion has focused on the mechanical details of how the matrix equations of the complex Kohn variational method are set up. The foregoing discussion makes it clear that the formulation admits the use of multiconfiguration target wave functions and large-scale optical potentials and that modern electronic structure techniques can be used to carry out most of the manipulations required quite efficiently. We wish to emphasize, however, that the partitioning of P -space and Q -space terms and the appropriateness of certain configurations is ultimately dictated by physical consideration of the underlying approximations. In this study, we have restricted the calculations to collision energies where only two channels are energetically open. As we shall see, the inclusion of CI relaxation terms in the optical potential is critical in determining the resonance features in the excitation cross sections over this range of energies. However, because of the discrete nature of the optical potential (it is constructed from the inverse of a finite matrix), we would expect to encounter numerous pseudoresonances if the calculations were arbitrarily extended to higher energies. These pseudoresonances are not associated with the numerical method being used, but rather, are a result of the inconsistencies caused by the neglect of open channels. For meaningful calculations at intermediate energies, special care is required if multiconfiguration target states and/or optical potential terms are to be used. These considerations are beyond the scope of the present study and will be addressed elsewhere [22].

D. Separable expansions

The electronic structure codes provide an efficient mechanism for evaluating matrix elements of the two component parts of H_{PP} and V_{opt} over the space of bound orbitals used in the expansion of the channel scattering functions. For evaluation of the bound-free

and free-free matrix elements, we rely on numerical quadrature techniques. The adaptive three-dimensional (3D) quadrature scheme we employ has been previously described in detail [4] and will not be repeated here. What we want to emphasize here is that this type of an approach is only used for direct-type continuum matrix elements of H_{PP} which, as we have previously shown, can be reduced to a single 3D quadrature of various one-electron transition potentials. Exchange-type matrix elements of H_{PP} and matrix elements of V_{opt} involving continuum orbitals are considerably more difficult. The fact is that we never have to compute them. By invoking separable approximations to the operators in question, this neglect can be made rigorous [12]. In this section we outline the arguments needed to justify this simplification.

A separable representation of an operator can be achieved by projection onto a finite basis:

$$H \approx \sum_{\alpha, \beta} |\varphi_\alpha\rangle H_{\alpha\beta} \langle \varphi_\beta| . \quad (17)$$

With reference to the effective Hamiltonian defined in Eq. (6), this type of representation is invoked for the exchange components of H_{PP} , as well as V_{opt} . The basis we use for this separable representation is the set of target orbitals, along with the square-integrable functions used to expand the channel orbitals $F_{\Gamma\Gamma_0}$. Because the continuum functions f_i^Γ and g_i^Γ used in the calculation are orthogonal to this entire set of basis functions by construction, then all matrix elements of H_{PP}^{exch} and V_{opt} involving continuum functions will vanish and the entire effect of exchange and electron-target correlation will be carried in the bound-bound matrix elements. Whether or not this is a good approximation depends upon how many functions we include in the underlying L^2 basis and how close it comes to being complete for the purpose of representing the operators in question. In this context, one must bear in mind that orbitals used in the determination of target wave functions must necessarily be excluded from the set of L^2 functions used to expand the channel scattering functions. There is no formal difficulty here, since these target orbitals, as we have stated, appear in appropriate $(N+1)$ -electron “penetra-

tion” terms in Q space. However, because the optical potential is only represented in separable form, the transference of terms from P space to Q space does involve an approximation. For this reason, we try to keep the target orbital space as compact as possible. The use of natural orbitals is ideal in this regard [23]. It is, nonetheless, difficult to quantify the magnitude of the errors attributed to the separable representation of V_{opt} . Ultimately, this quantification must be done empirically and it is therefore very important to carry out calculations with several difficult choices of basis sets in the course of a particular study.

III. CALCULATIONS

A. Fixed-nuclei cross sections

There are three electronic states of HeH^+ that are relevant to the present study, the ground $X^1\Sigma^+$ state and the first two excited states of $^3\Sigma^+$ and $^1\Sigma^+$ symmetry, respectively. The ground state, which is bound by ~ 2 eV, has an equilibrium separation of 0.77 \AA [24] and dissociates to $\text{He} + \text{H}^+$, while the excited states are both repulsive and dissociate to $\text{He}^+ + \text{H}$. The three states are nominally described by the single configurations: $(1\sigma^2), X^1\Sigma^+$, $(1\sigma 2\sigma), ^1^3\Sigma^+$, and $(1\sigma 2\sigma), 2^1\Sigma^+$. Extensive calculations with multiconfiguration wave functions have been carried out on this system by Green *et al.* [25] and were used as a guide in checking the accuracy of the target wave functions we employed in our study.

The target wave functions we used were obtained from CI calculations carried out in a basis of Gaussian functions given in Table I. An initial set of computations was carried out at the ground-state equilibrium geometry. We first performed full CI calculations and extracted natural orbitals from the average of the one-particle density matrices for the three lowest states. These natural orbitals enable us to provide a more compact representation of the target wave functions [23]. The final “target basis” we chose consisted of the six natural orbitals with the largest occupation numbers—corresponding to the 1σ and 2σ orbitals that describe the dominant configurations for the states in question, along with one additional π and

TABLE I. Exponents of Cartesian Gaussian basis used in target and scattering calculations.

Center		Exponents
Target basis		
Hydrogen	s type	48.4479 7.283 46, 1.651 39, 0.462 447, 0.145 885, 0.07
Hydrogen	p type	1.0, 0.2 0.031 25
Helium	s type	414.466, 62.2492, 14.2212, 4.038 78, 1.297 19, 0.447 530, 0.160 274
Helium	p type	1.0, 0.2, 0.05
Bond center	s type	0.083, 0.027, 0.0093
Bond center	p type	0.19, 0.0655, 0.0226 0.007 79
Supplemental scattering basis		
Hydrogen	p type	70.0, 21.0, 7.0
Helium	p type	210.0, 70.0, 21.0, 7.0
Bond center	s type	0.10, 0.05

two σ compact natural orbitals needed for correlation. The final target wave functions used in the scattering calculations were obtained from a full CI calculation in this smaller basis of natural orbitals. The excitation energies we obtained in this truncated basis were 21.423 and 26.216 eV and compare very favorably with the results obtained in the full virtual orbital basis (21.441 and 26.117 eV).

The target basis was augmented with additional Gaussian functions to provide flexibility in describing the scattering wave function. This set is also given in Table I. To test the adequacy of this basis, we also carried out calculations at several energies with larger basis sets than those used here and found the results to change by less than 10%. The $X^1\Sigma^+ \rightarrow 1^3\Sigma^+$ transition is spin forbidden and the corresponding excitation cross section converges rapidly in l . Since calculations were performed at energies where only the ground and $^3\Sigma^+$ states were open, it was only necessary to include continuum basis functions up to $l=6$ for satisfactory convergence.

To relax any orthogonality constraints on the trial wave function imposed by orthogonalizing the continuum functions f_l^Γ and g_l^Γ to the orbitals used to expand the target states, we included in Q space all possible $(N+1)$ -electron configurations, consistent with the total space/spin symmetry, in which only natural orbitals are occupied. The optical potential also included CI relaxation terms as described in Sec. II C. In this case, the optical potential included all relaxation terms which could be constructed as the direct product of an excited target eigenstate χ_i ($i \neq 1, 2$) and a scattering orbital although, as we have pointed out, the projection operator scheme we employ obviates the need for explicit construction of the excited target eigenstates. In computing total excitation cross sections, we included contributions from $^2\Sigma^+$ and $^2\Pi$ total symmetry.

Figures 1 and 2 depict the $^2\Sigma^+$ and $^2\Pi$ contributions to the $X^1\Sigma^+ \rightarrow 1^3\Sigma^+$ excitation cross sections, respectively, calculated at the equilibrium internuclear separation of

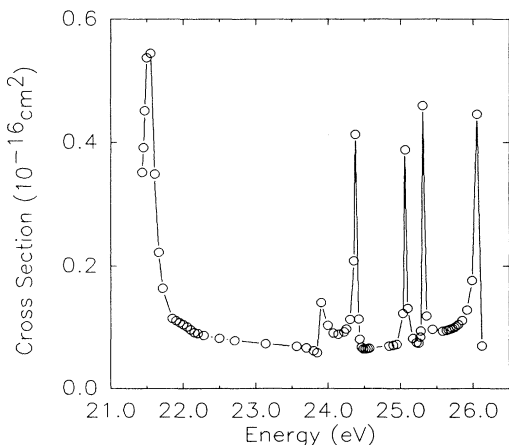


FIG. 1. Theoretical $X^1\Sigma^+ \rightarrow 1^3\Sigma^+$ excitation cross section in overall $^2\Sigma^+$ symmetry calculated at the equilibrium HeH⁺ internuclear separation.

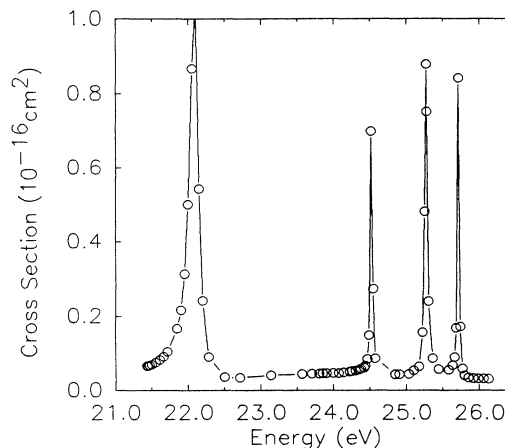


FIG. 2. As in Fig. 1, for $^2\Pi$ symmetry.

0.77 Å. Both the $^2\Sigma^+$ and $^2\Pi$ cross-section components are dominated by a series of sharp resonances superimposed on a relatively flat background. The magnitude of the total background excitation cross section is approximately 10^{-17} cm². By analyzing the structure of the trial wave function in the vicinity of the various resonances, we were able to determine that all the peaks, with the exception of the $^2\Sigma^+$ peak at 24 eV, are Feshbach resonances [26] associated with the energetically closed $2^1\Sigma^+$ state of HeH⁺; i.e., the resonances are of the form

$$(1\sigma 2\sigma)^1 n \sigma, ^2\Sigma^+, (1\sigma 2\sigma)^1 n \pi, ^2\Pi.$$

The $^2\Sigma^+$ resonance at 24 eV is broader than the other resonances and has a high-energy tail which overlaps the next $^2\Sigma^+$ resonance, as well as the second $^2\Pi$ resonance. Analysis of the trial wave function showed this to be a core-excited shape resonance [26] of the form $(1\sigma 2\sigma)^3 n \sigma, ^2\Sigma^+$.

Figure 3 shows the total fixed-nuclei cross section; the experimental results of Yousif and Mitchell [1], taken under low extraction conditions, are shown in the Fig. 3 inset. These results taken along would appear to support the qualitative picture of a relatively flat excitation cross section with a number of sharp resonance peaks superimposed. However, we shall see that a consideration of the nuclear dynamics will modify these results.

B. Effect of nuclear motion

The excited $1^3\Sigma^+$ and $2^1\Sigma^+$ states of HeH⁺ are both steeply repulsive near 0.77 Å and consequently the vertical excitation energies from the ground state are sensitive to small displacements of the internuclear separation from the equilibrium value. One might expect the HeH⁺ resonance states to track their parent ion states to first order and the resonance energies to correspondingly shift as the internuclear distance is changed. This will result in a characteristic broadening of the resonance peaks in the observed cross sections which can be quantified as follows.

On the assumption that the rotational levels of the tar-

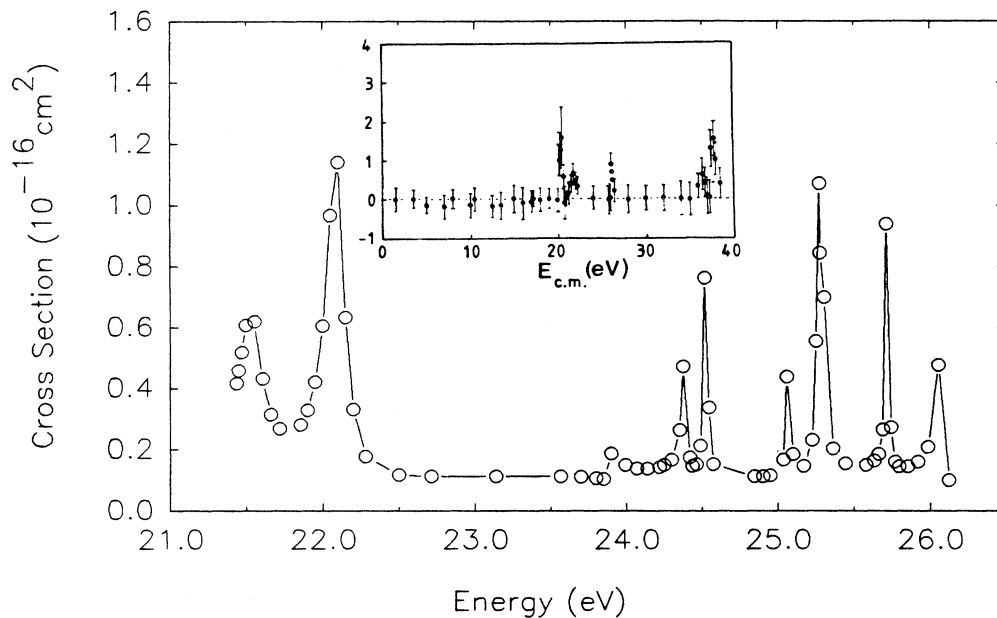


FIG. 3. Total $X^1\Sigma^+ \rightarrow 1^3\Sigma^+$ excitation cross section calculated at $R=0.77 \text{ \AA}$. The inset shows measured dissociative excitation cross sections for HeH^+ (Ref. [1]) under low-extraction conditions where no hot bands are present.

get can be taken to be essentially degenerate, the rotationally averaged excitation cross section, summed over final states and averaged over initial states, takes the form

$$\sigma_{v_0 \rightarrow k_v} = \frac{k_v}{k_0} \int \left| \int \chi_{v_0}(R) f(E_0; R, \Omega) \chi_{k_v}(R) dR \right|^2 \frac{1}{4\pi} d\Omega \quad (18)$$

where χ_{v_0} and χ_{k_v} are the initial and final (continuous) target vibrational wave functions, f is the body-fixed scattering amplitude, and Ω denotes the spherical polar angles of the molecular axis relative to the laboratory fixed axes. If we use the classical δ -function approximation to replace the final continuum vibrational function by $|dV/dR|^{-1/2} \delta(R - R_0^k)$ where R_0^k is the classical turning point on the upper-state potential curve V , then the total excitation cross section is simply given as

$$\begin{aligned} \sigma(E_0) &= \frac{4\pi}{k_0^2} \sum_{l,l',m} \int |\chi_{v_0}(R) T_{ll'm}(R)|^2 dR \\ &\equiv \int \sigma(E_0, R) \chi_{v_0}(R)^2 dR, \end{aligned} \quad (19)$$

that is, as the convolution of the “fixed-nuclei cross section” with the square of the initial vibrational wave function.

The ground-state vibrational frequency of HeH^+ is 3328 cm^{-1} [24], corresponding to zero point vibrational motion of approximately $R_0 \pm 0.1 \text{ \AA}$. Theoretical calculations indicated that the excited $^3\Sigma^+$ and $^1\Sigma^+$ target state energies change by more than 5 eV over this range of internuclear separation. To test the sensitivity of the cross section to changes in the He–H distance, we repeated the calculations in $^2\Sigma^+$ symmetry at $R_0 \pm 0.05 \text{ \AA}$. We

found the resonance positions to shift by roughly the same amount as the $X^1\Sigma^+ - 2^1\Sigma^+$ excitation energy, as expected, but the resonance widths, as well as the background cross-section values, to change very little. Therefore for the purpose of evaluating Eq. (19) we simply used the total cross-section values calculated at R_0 , shifted to reflect the R dependence of the excitation thresholds. The vibrational wave function was approximated by a harmonic oscillator function. Figure 4 shows the vibrational averaged total cross section. As one would expect, the resonance peaks do not survive the vibrational averaging and what is obtained is the smooth background value. It is unlikely that the use of more accurate initial- and/or final-state vibrational wave functions would substantially change this result.

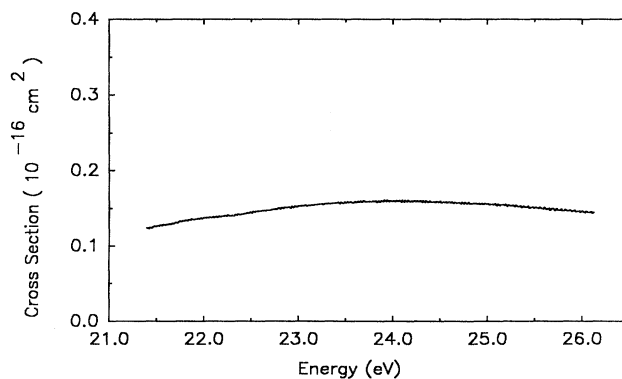


FIG. 4. Total excitation cross section, averaged over the vibrational motion of ground state.

IV. DISCUSSION

We used the complex Kohn variational method to compute cross sections for the dissociative excitation of HeH⁺. These calculations employed multiconfiguration correlated target wave functions, and used an *ab initio* optical potential to include the effects of closed channels. The fixed-nuclei cross sections were found to be dominated by a series of sharp resonances, in apparent agreement with recent experimental findings. However, because the resonance states were found to parallel their steeply repulsive ionic parent states, the final cross sections we obtained, averaged over the vibrational motion of the initial state, were structureless.

Yousif and Mitchell speculated that the sharp structures they observed might correspond to doubly excited resonant neutral states and stated that similar structures have been seen in measurements on N₂⁺ [27] and H₃⁺ [28]. However, we have shown here that the presence of such structures in the fixed-nuclei cross sections will not manifest itself in the observable cross section unless these states are relatively independent of internuclear separation in the Franck-Condon region. Our calculations indicated that this is not the case. We even performed more extensive calculations on the HeH* neutral states in which the core orbitals were allowed to relax, but we found no resonance states that did not simply parallel the excited target ion state.

The finite basis we have employed in our calculations is only capable of describing the lowest members in an infinite Rydberg series of resonances converging on an excited singlet state of HeH⁺. For the higher members of this series, the Born-Oppenheimer separation of electronic and nuclear motion must necessarily break down. We therefore conclude that the structures seen by Mitchell and Yousif might arise from nonadiabatic effects associated with these highly excited resonance states.

A notable feature of these calculations was the use of natural orbitals to achieve a compact representation of the target wave function. In this case, it was possible to use a full CI description of the target states, thus avoiding the usual issues of balance between the *N*- and (*N*+1)-electron problems and recorelation that often occur in scattering calculations. The approach we have used here would be especially useful in polyatomic systems like H₃⁺, where more states are involved in the excitation process and the description of the scattering from these states has to be carried out in a balanced fashion.

ACKNOWLEDGMENTS

This work was performed under the auspices of the U.S. Department of Energy at Lawrence Livermore National Laboratory under Contract No. W-7405-Eng-48. A.E.O. acknowledges support of the National Science Foundation, Grant No. PHY-90-14845.

-
- [1] F. B. Yousif and J. B. A. Mitchell, *Phys. Rev. A* **40**, 4318 (1989).
- [2] B. I. Schneider and T. N. Rescigno, *Phys. Rev. A* **37**, 3749 (1988).
- [3] A. E. Orel, T. N. Rescigno, and B. H. Lengsfeld III, *Phys. Rev. A* **42**, 5292 (1990).
- [4] C. W. McCurdy and T. N. Rescigno, *Phys. Rev. A* **39**, 4487 (1989).
- [5] S. D. Parker, C. W. McCurdy, T. N. Rescigno, and B. H. Lengsfeld III, *Phys. Rev. A* **43**, 3514 (1991).
- [6] W. Eisner and M. J. Seaton, *J. Phys. B* **5**, 2187 (1972).
- [7] M. Gailitis, in *Effective Cross Sections for the Collisions of Electrons with Atoms: Atomic Collisions III*, edited by V. I. Veldre (Latvian Academy of Science, Riga, 1965).
- [8] P. G. Burke and A. J. Taylor, *Proc. Phys. Soc. London* **88**, 549 (1966).
- [9] T. N. Rescigno and A. E. Orel, *Phys. Rev. A* **43**, 1625 (1991).
- [10] Y. Sun, D. J. Kouri, D. G. Truhlar, and D. W. Schwenke, *Phys. Rev. A* **41**, 4857 (1990).
- [11] R. K. Nesbet, *Variational Methods in Electron-Atom Scattering* (Plenum, New York, 1980).
- [12] T. N. Rescigno and B. I. Schneider, *Phys. Rev. A* **37**, 1044 (1988).
- [13] D. G. Truhlar, J. Abdallah, and R. L. Smith, *Adv. Chem. Phys.* **25**, 211 (1974).
- [14] H. E. Saraph, M. J. Seaton, and J. Shemming, *Proc. Phys. Soc. London* **89**, 27 (1966); P. G. Burke, A. Hibbert, and W. D. Robb, *J. Phys. B* **4**, 153 (1971).
- [15] H. Feshbach, *Ann. Phys. (N.Y.)* **5**, 357 (1958); **19**, 287 (1962).
- [16] E. R. Davidson, *J. Comput. Phys.* **17**, 87 (1975); P. E. M. Siegbahn, *J. Chem. Phys.* **70**, 5391 (1980); **72**, 1647 (1980).
- [17] B. I. Schneider, B. H. Lengsfeld III, and T. N. Rescigno (unpublished).
- [18] B. H. Lengsfeld III, T. N. Rescigno, and C. W. McCurdy, *Phys. Rev. A* (to be published).
- [19] S. Weiguo, C. W. McCurdy, and B. H. Lengsfeld III (unpublished).
- [20] B. H. Lengsfeld III and B. Liu, *J. Chem. Phys.* **75**, 478 (1981).
- [21] J. A. Pople, R. Krishnam, H. B. Schlegel, and J. S. Binkley, *Int. J. Quantum Chem. Symp.* **13**, 225 (1979).
- [22] B. H. Lengsfeld III and T. N. Rescigno, *Phys. Rev. A* (to be published).
- [23] See, for example, R. McWeeny and B. T. Sutcliffe, *Methods of Molecular Quantum Mechanics* (Academic, New York, 1969).
- [24] K. P. Huber and G. Herzberg, *Molecular Spectra and Molecular Structure IV. Constants of Diatomic Molecules* (Van Nostrand Reinhold, New York, 1979).
- [25] T. A. Green, H. H. Michels, J. C. Browne, and J. A. Madson, *J. Chem. Phys.* **61**, 5186 (1974); T. A. Green, H. H. Michels, and J. C. Browne, *ibid.* **69**, 101 (1978).
- [26] G. J. Schulz, *Rev. Mod. Phys.* **45**, 378 (1973).
- [27] C. Norem, F. B. Yousif and J. B. A. Mitchell, *J. Chem. Soc. Faraday Trans. 2* **85**, 1697 (1989).
- [28] J. B. A. Mitchell (private communication).